


Prss56, a novel marker of adult neurogenesis in the mouse brain

Alexandre Jourdon^{1,2} · Aurélie Gresset¹ · Nathalie Spassky¹ · Patrick Charnay¹  · Piotr Topilko¹ · Renata Santos¹

Received: 30 April 2015 / Accepted: 7 December 2015 / Published online: 23 December 2015
© Springer-Verlag Berlin Heidelberg 2015

Abstract Adult neurogenesis in the mammalian brain is restricted to specific regions, such as the dentate gyrus (DG) in the hippocampus and the subventricular zone (SVZ) in the walls of the lateral ventricles. Here, we used a mouse line carrying a knock-in of Cre recombinase in the *Prss56* gene, in combination with two Cre-inducible fluorescent reporters (*Rosa26^{mTmG}* and *Rosa26^{tdTom}*), to perform genetic tracing of *Prss56*-expressing cells in the adult brain. We found reporter-positive cells in three neurogenic niches: the DG, the SVZ and the hypothalamus ventricular zone. In the prospective DG, *Prss56* is expressed during embryogenesis in a subpopulation of radial glia. The pattern of migration and differentiation of reporter-positive cells during development recapitulates the successive steps of DG neurogenesis, including the formation of a subpopulation of adult neural stem cells (NSC). In the SVZ, *Prss56* is expressed postnatally in a subpopulation of adult NSC mainly localized in the medial-ventral region of the lateral wall. This subpopulation preferentially gives rise to deep granule and Calbindin-positive periglomerular interneurons in the olfactory bulb. Finally, *Prss56* is also expressed in a subpopulation of $\alpha 2$ -tanyocytes, which are potential adult NSCs of the hypothalamus ventricular zone.

Our observations suggest that some $\alpha 2$ -tanyocytes translocate their soma into the parenchyma and may give rise to a novel cell type in this territory. Overall, this study establishes the *Prss56^{Cre}* line as an efficient and promising new tool to study multiple aspects of adult neurogenesis in the mouse.

Keywords Adult neurogenesis · Neural stem cell · Subventricular zone · Olfactory bulb · Dentate gyrus · Hypothalamus · Tanyocyte

Introduction

Neurogenesis persists throughout life in mammals in two major neurogenic niches: the subgranular zone (SGZ) of the dentate gyrus (DG) in the hippocampus, and the subventricular zone (SVZ) in the walls of the lateral ventricles (Altman and Das 1965a; Lois and Alvarez-Buylla 1994). More recently, adult neurogenesis has also been observed in other regions of the brain, such as the hypothalamus in rodents (Kokoeva et al. 2005; Pierce and Xu 2010; Robins et al. 2013a) and the striatum in humans (Ernst et al. 2014).

The general organization of adult SGZ and SVZ germinal niches are similar (reviewed in Ihrie and Álvarez-Buylla 2011; Ming and Song 2011; Gage and Temple 2013). Cells with astroglial properties behave as neural stem cells (NSC), generating intermediate progenitors (also called transient amplifying progenitors) by asymmetric division. These progenitors divide and give rise to neuroblasts that continue to proliferate, migrate and differentiate into neurons. In the DG, the neuroblasts migrate into the granular layer and mature into excitatory granule neurons. In the SVZ, the neuroblasts migrate over long distances along the rostral migratory stream (RMS) to the

Electronic supplementary material The online version of this article (doi:10.1007/s00429-015-1171-z) contains supplementary material, which is available to authorized users.

✉ Patrick Charnay
patrick.charnay@ens.fr

¹ Ecole Normale Supérieure, PSL Research University, CNRS, Inserm, Institut de Biologie de l'Ecole Normale Supérieure (IBENS), 46 rue d'Ulm, 75005 Paris, France

² UPMC Univ Paris 06, IFD, Sorbonne Universités, 4 Place Jussieu, 75252 Paris Cedex 05, France

olfactory bulb (OB). In the OB, they differentiate into two major types of interneurons: periglomerular cells (PGC) in the glomerular layer, and granule cells (GC) in the granule cell layer. Adult-born neurons integrate into pre-existing circuits of the DG and OB, but exhibit electrophysiological properties different from those of their embryonic counterparts until they have reached complete maturation (Espósito et al. 2005; Ge et al. 2007; Marín-Burgin et al. 2012; Deshpande et al. 2013). Although only a small subpopulation of neurons are generated postnatally, their enhanced synaptic plasticity confers on the adult circuitry the ability to evolve in response to experience, without affecting the circuitry's general stability (Ge et al. 2007; Lepousez et al. 2014). Adult neurogenesis in these niches is thus essential for some forms of learning, memory and mood regulation (Zhao et al. 2008).

Several studies have also reported the existence of neural stem/progenitor cells and neurogenesis in the adult hypothalamus (Pencea et al. 2001; Markakis et al. 2004; Kokoeva et al. 2005; Xu et al. 2005; Pierce and Xu 2010; Robins et al. 2013a). Since the hypothalamus is a master regulator of neuroendocrine function, this finding suggests that the integration of newborn neurons may affect the control of basic physiological functions, such as feeding. Indeed, blocking adult neurogenesis in the medial-basal hypothalamus results in altered weight and metabolic activity in adult mice (Lee et al. 2012). In this part of the hypothalamus, the third ventricle is lined dorsally by ciliated ependymal cells and ventrally by non-ciliated radial glial-like cells, termed tanycytes. The tanycytes constitute a heterogeneous population divided into four subtypes ($\alpha 1$, $\alpha 2$, $\beta 1$ and $\beta 2$) depending on the dorsal–ventral position of the cell bodies, projection of the basal processes, and expression of specific markers (Rodríguez et al. 2005; Haan et al. 2013; Robins et al. 2013a). Recent studies, based on fate mapping and functional characterization, have revealed that populations of $\alpha 2$ and $\beta 2$ tanycytes self-renew and generate glial and neuronal derivatives (Lee et al. 2012; Haan et al. 2013; Robins et al. 2013a). However, the cellular pathways involved in this process are still unknown.

Rapid progress in the understanding of adult NSC properties and functions has been made possible by the development of new tools, such as proliferation markers, viral vectors and conditional mutant mice (Gage and Temple 2013; Enikolopov et al. 2015). However, additional specific markers are still needed to address many issues, old and recent, concerning adult neurogenesis. The *Prss56* gene (previously named *L20*) encodes a potentially secreted trypsin-like serine protease involved in eye development in mice and humans, although its precise function has not been elucidated so far (Gal et al. 2011; Nair et al. 2011). We have shown that *Prss56* is expressed

in neural crest-derived boundary cap cells during mouse embryonic development (Coulpier et al. 2009). To investigate the fate of *Prss56*-expressing cells, we have generated a knock-in allele, *Prss56^{Cre}*, carrying Cre recombinase in the locus (Gresset et al. 2015). Combination of this allele with Cre-activable reporter constructs allows tracing of *Prss56*-expressing cells and their derivatives. Unexpectedly, in the postnatal brain, reporter-positive cells were found specifically in several neurogenic niches, including the SGZ, the SVZ, and the lateral wall of the hypothalamus. In the developing DG, we observe that *Prss56* is expressed in a subpopulation of radial glia from embryonic day (E) 13.5 in the dentate ventricular zone. The pattern of migration and differentiation of their derivatives faithfully recapitulates the successive steps of morphogenesis and neurogenesis of the DG, indicating that these cells participate in its formation. In the SVZ, *Prss56* is expressed postnatally in a ventral subpopulation of NSCs and the *Prss56^{Cre}* allele allows tracing of their derivatives through the RMS to the OB, where they preferentially differentiate into deep GCs and Calbindin (CalB)-positive PGCs. Finally, in the hypothalamus, *Prss56* is expressed in $\alpha 2$ type tanycytes that proliferate, translocate their soma into the parenchyma, and are likely to generate neurons or glia in the arcuate and dorsal-medial nuclei in the adult. The newly-generated *Prss56^{Cre}* mouse line therefore appears to be a powerful genetic tool to further study the development, the organization, and the functions of postnatal neurogenic niches.

Materials and methods

Animals

The *Prss56^{Cre}* mouse line was generated by insertion of the Cre recombinase coding sequence immediately after the ATG start codon of the *Prss56* gene (Gresset et al. 2015). Genotyping was performed by PCR using DNA extracted from the tail and the following primers: 5'-CAGGTGAGGTGCGGACCATT-3', 5'-ACGGAATCCATCGCTCGACCAGTT-3' and 5'-AAACCACTGCCACCGCAT-3'. *Prss56^{Cre/Cre}* homozygous animals are viable and fertile. The other mouse lines, as well as their genotyping, were described previously: *hGfap::GFP* (Nolte et al. 2001), *Rosa26^{mTmG}* (Muzumdar et al. 2007) and *Rosa26^{tdTom}* (Madisen et al. 2010). All lines were maintained in a mixed *C57BL/6/DBA/2* background. Brains were extracted after transcardiac perfusion with 4 % paraformaldehyde, then post-fixed in the same solution overnight at 4 °C and sectioned with a vibratome. When required, vibratome sections were kept in storage buffer

(30 % glycerol, 30 % ethylene glycol in sodium phosphate buffer) at -20°C until further processing. Lateral wall whole-mounts were prepared as described and fixed in 4 % paraformaldehyde in phosphate buffered saline solution (PBS) at 4°C for 3 h (Mirzadeh et al. 2010). Mice housing and breeding, euthanasia and experimental procedures were performed in accordance with the Council of European Union directive of 22 September 2010 (2010/63/UE) and approved by the French Ethical Committee (Project No. B750520).

Immunohistochemistry and imaging

Vibratome sections (50–150 μm) and whole-mounts were blocked for 1 h at room temperature with 10 % fetal bovine serum, 0.3 % Triton X-100 in PBS. Primary antibodies were incubated in the same solution overnight at 4°C and secondary antibodies were incubated for 3 h at room temperature in 1 % fetal bovine serum, 0.3 % Triton X-100 in PBS solution. Sections were counterstained with Hoechst 33342 (Sigma) for nuclei detection. The following primary antibodies were used: mouse anti-APC (1/500, Abcam); rat anti-BrdU (1/100, AbCys); rabbit anti-BLBP (1/200, Millipore); mouse anti-CalB (1/500, Swant); goat anti-CalR (1/500, Swant); mouse anti- β -catenin (1/200, BD Transduction); goat anti-DCX (1/300, Santa Cruz); rabbit anti-dsRed (1/400, Clontech); mouse anti-GFAP (1/100, Millipore); rabbit anti-GFAP (1/300, Dako); rabbit anti-GFP (1/500, Invitrogen); rat anti-GFP (1/500, Nacalai Tesque); mouse anti-HuC/D (5 $\mu\text{g}/\text{mL}$, Molecular Probes); mouse anti-Nestin (1/100, Millipore); mouse anti-NeuN (1/800, Millipore); rabbit anti-NG2 (1/200, Millipore); goat anti-NeuroD (1/400, Santa Cruz Biotechnology); goat anti-Prox1 (1/400, R&D Systems); mouse anti-S100 (1/500, Sigma); goat anti-Sox2 (1/200, Santa Cruz Biotechnology); goat anti-Sox10 (1/100, Santa Cruz Biotechnology); mouse anti-TH (1/1000, Millipore); mouse anti- β III-tubulin (1/600, Millipore); mouse anti- γ -tubulin (1/500, Sigma); chicken anti-Vimentin (1/100, Millipore). Secondary antibodies labeled with Cy3, Cy5, Alexa488, Alexa597 and Alexa647 were from Jackson Immuno Research and Molecular Probes. Sections were mounted in Fluoromount (SouthernBiotech). Images were acquired on Leica SP5 and SP8 confocal microscopes. Image processing and analysis were performed using ImageJ and Adobe Photoshop software. Cell counting data in the SVZ, RMS, OB and DG regions involved the analysis of at least three different confocal stacks per region and per animal. Co-localization with different markers was confirmed by the analysis of sequential single optical slices.

In situ hybridization and BrdU labeling

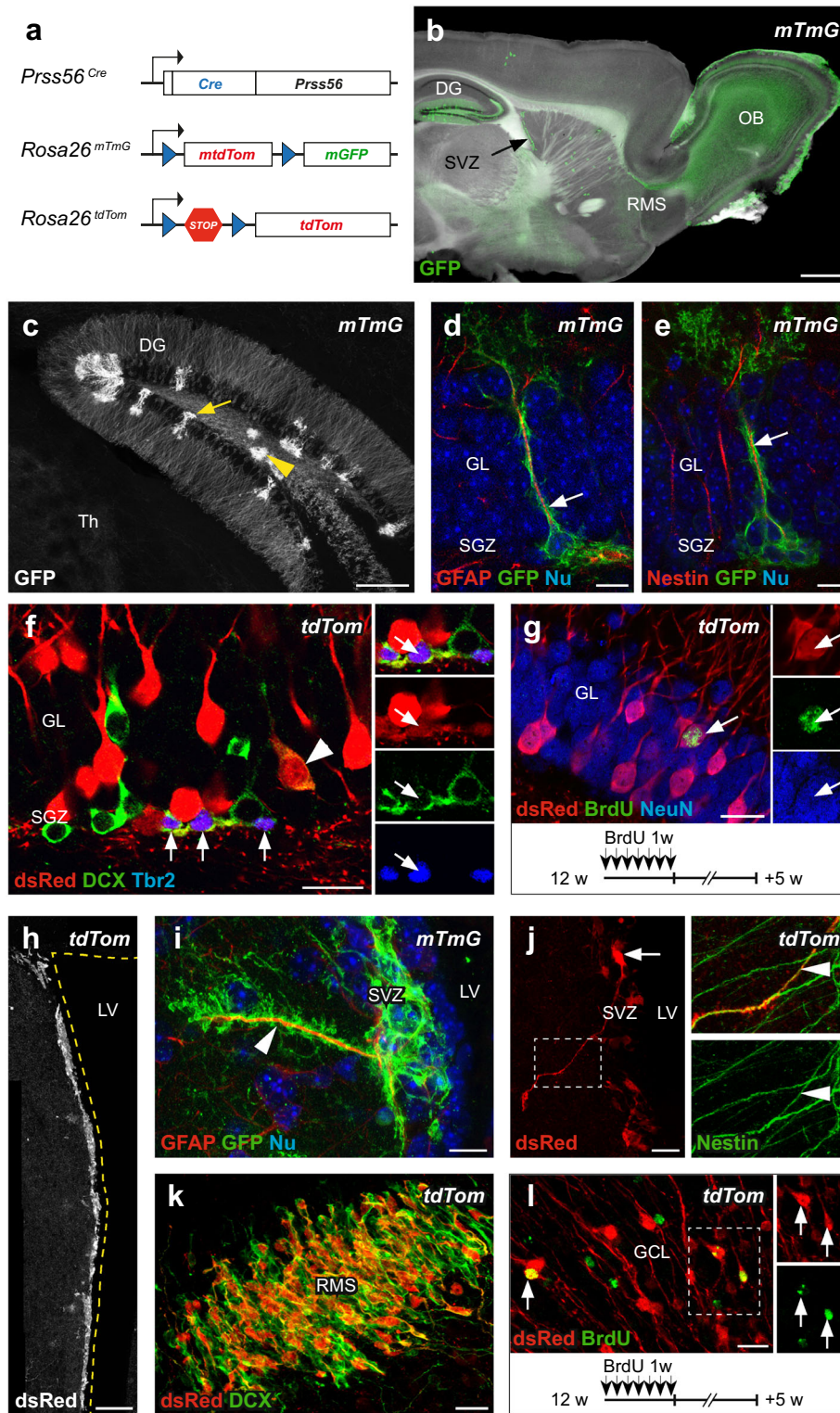
mRNA in situ hybridization was performed on brain vibratome sections (150 μm) from wild type and *Prss56^{Cre}* animals using digoxigenin-labeled RNA probes synthesized by PCR as described previously (Coulpier et al. 2009). For BrdU labeling, 3 month-old mice received daily intraperitoneal injections of 5-bromodeoxyuridine (BrdU, Sigma) in saline solution at 50 mg/kg/day for 7 days. The chase periods were either 5 or 12 weeks after the last injection and 3–4 animals were analyzed per group. For BrdU immunodetection, sections were pre-treated with 2 N HCl at 37°C for 30 min before primary antibody labeling. FGF and BrdU infusions were performed as described (Robins et al. 2013a). In brief, 3 month-old mice were implanted with a steel guide cannula to reach the right lateral ventricle using the following stereotaxic coordinates: Bregma, AP: -0.5 mm; L: $+1.2$ mm; DV: -2.5 mm. Osmotic pumps (Alzet) were installed and filled with artificial cerebrospinal fluid containing 1 mg/mL mouse serum Albumin (Sigma), 1 mg/mL BrdU and 60 $\mu\text{g}/\text{mL}$ bFGF (Sigma). The solution was released for 7 days in the lateral ventricle. Mice were killed 6 weeks after the beginning of the infusion.

Results

Fate mapping of *Prss56*-expressing cells in the neurogenic niches of the adult brain

To identify *Prss56*-expressing cells and their progeny in the adult brain, we first introduced the knock-in *Prss56^{Cre}* allele (Gresset et al. 2015; Fig. 1a) into the *Rosa26^{mTmG}* reporter line, in which Cre recombination leads to permanent expression of membrane-targeted enhanced green fluorescent protein (Muzumdar et al. 2007). Analysis of parasagittal sections through *Prss56^{Cre/+}, Rosa26^{mTmG/+}* adult brain revealed the presence of mGFP-positive cells in two neurogenic niches, the DG and the SVZ, as well as in the RMS and the OB (Fig. 1b). We therefore investigated whether these mGFP-positive cells participate in adult neurogenesis.

In the DG, we observed different types of labeled cells, including neurons, NSCs and astrocytes (Fig. 1c; Supplemental Fig. 1a). Most mGFP-positive cells show low levels of fluorescence and correspond to granule neurons, with their cell bodies in the granular layer, dendrites in the molecular layer, and a single axon extending to CA3 through the hilus (Fig. 1c; Supplemental Fig. 1a, b'). More highly fluorescent cells, showing a radial morphology, a cell body located in the SGZ, a radial process extending



through the granular layer, and dense arborization in the molecular layer, express glial fibrillary acidic protein (GFAP) and Nestin, two markers of NSCs (Fig. 1d, e;

Supplemental Fig. 1b, b'). These cells are likely to correspond to the so-called type I NSCs of the DG (Kempermann et al. 2004). Another population of highly fluorescent

Fig. 1 Tracing of *Prss56*-expressing cell derivatives in the adult brain. **a** Schematic representation of the *Prss56*^{Cre}, *Rosa26*^{mTmG} and *Rosa26*^{tdTom} alleles. **b** Parasagittal section through an adult *Prss56*^{Cre/+}, *Rosa26*^{mTmG/+} brain, revealing labeled (green) cells in the DG, SVZ, RMS and OB. Also note the presence of labeled olfactory ensheathing cells at the periphery of the bulb. **c** Coronal section through an adult *Prss56*^{Cre/+}, *Rosa26*^{mTmG/+} DG, showing the presence of labeled type I NSCs (arrow), astrocytes (arrowhead) and granule neurons (weakly fluorescent, mostly identifiable by their axons and dendrites). **d, e** Optical slices of a confocal z-stack showing that labeled (green) type I NSCs express GFAP (**d**, arrow) and Nestin (**e**, arrow). **f** Optical slice through an adult *Prss56*^{Cre/+}, *Rosa26*^{tdTom/+} DG, showing tdTom-positive transient amplifying progenitor cells that are Tbr2- and DCX-positive (arrows) and a tdTom-, DCX-positive neuroblast (arrowhead). Separated channels are shown on the right at the level of the Tbr2-positive cells. **g** Optical slice through a *Prss56*^{Cre/+}, *Rosa26*^{tdTom/+} DG, showing a tdTom-, NeuN-positive granule neuron that incorporated BrdU during adulthood (arrow). The BrdU injection protocol is illustrated below and separated channels at the level of the BrdU-positive cell are shown on the right. **h** Coronal confocal image from a *Prss56*^{Cre/+}, *Rosa26*^{tdTom/+} brain showing tdTom-positive cells in the SVZ (the limit of the lateral ventricle is indicated by the dotted line). **i, j** Confocal images of labeled (green in **i** and red in **j**) B1 cells in the SVZ showing the cell body close to the ependymal layer (arrow in **j**) and the long extension into the striatum (arrowheads). These cells express GFAP (**i**, arrowhead) and Nestin (**j**, arrowhead). Note the absence of mGFP in ependymal cells in **i**. **k** Confocal stack of the RMS, showing tdTom-, DCX-positive neuroblasts. **l** Coronal confocal optical slice of the OB, showing tdTom-positive neurons that have incorporated BrdU during adulthood. The BrdU injection protocol is illustrated below and separated channels are presented on the right. **DG** dentate gyrus, **GCL** granule cell layer of the OB, **GL** granular layer of the DG, **LV** lateral ventricle, **OB** olfactory bulb, **RMS** rostral migratory stream, **SGZ** subgranular zone, **SVZ** subventricular zone, **Th** thalamus. Scale bars 1 mm (**b**), 200 μm (**c**), 100 μm (**h**), 20 μm (**f, g, j-l**) and 10 μm (**d, e, i**)

cells, observed in the molecular layer and hilus, show morphologies consistent with astrocytic identity (Fig. 1c; Supplemental Fig. 1a).

Labeling of transient amplifying progenitors and neuroblasts was difficult to establish because of the membrane localization of the GFP reporter. To circumvent this difficulty, we used another reporter, *Rosa26*^{tdTom}, for which Cre-mediated recombination results in the expression of cytoplasmic tandem dimer Tomato (tdTom, Fig. 1a; Supplemental Fig. 1c; Madisen et al. 2010). Using this reporter, together with a *hGfap::GFP* allele (Beckervordersandforth et al. 2010), we first confirmed that some of the *Prss56*^{Cre}-traced cells simultaneously express GFAP and Nestin (Supplemental Fig. 1d), establishing that they are type I NSCs. These cells express low levels of the tdTom reporter (Supplemental Fig. 1d). In addition, co-labeling for the markers T-box brain protein 2 (Tbr2) and doublecortin (DCX) indicated that transient amplifying progenitors (Tbr2-positive) and neuroblasts (DCX-positive) were among the tdTom-positive cells (Fig. 1f). To confirm that reporter-positive NSCs in the SGZ proliferate and give rise to new neurons in the adult brain, we performed BrdU labeling in 3 month-old mice. Five weeks

later, reporter-positive, BrdU-labeled neurons were identified in the DG, indicating that they were generated during adulthood (Fig. 1g). Taken together, our analyses indicate that our tracing system labels all the steps of the adult neurogenic and gliogenic pathway in the DG: adult NCSs, transient amplifying progenitors, neuroblasts, neurons, and astrocytes. Nevertheless, in the dorsal DG, *Prss56*^{Cre}-traced neurogenesis represents only a minor component of all neurogenic activity (11.3 ± 6.6 % of the BrdU-positive cells were tdTom-positive in the *Prss56*^{Cre/+}, *Rosa26*^{tdTom/+} granular layer, *n* = 3).

Tracing the progeny of *Prss56*-expressing cells in the adult brain also labeled the SVZ-RMS-OB neurogenic pathway (Fig. 1b, h–l). In the SVZ, we observed reporter-positive cells with astrocytic features expressing both GFAP and Nestin (Fig. 1i, j, and data not shown). Their cell bodies lie close to the ependymal cell layer, with a primary cilium contacting the ventricle and long basal processes often contacting blood vessels (Figs. 1i, j, 3f and data not shown). These cells are likely NSCs (named B1 cells in the SVZ). Ependymal cells were never labeled (Fig. 1i), indicating that the *Prss56* gene is not expressed in this population. In addition to NSCs, numerous reporter-positive neuroblasts expressing DCX and migrating in chains were identified in the SVZ (data not shown) and the RMS (Fig. 1k). Finally, reporter-positive interneurons were observed in different layers of the OB (Fig. 1b, l) and BrdU labeling confirmed that some of these neurons were generated during adulthood (Fig. 1l).

To compare our two reporter alleles and in particular to evaluate their relative efficiency of recombination, we generated animals carrying both reporters together with the Cre driver (*Prss56*^{Cre/+}, *Rosa26*^{tdTom/mTmG}) and analyzed the activation of the markers in the brain at P14 (Supplemental Fig. 1e–h). In the DG, the SVZ and the RMS, we found that most labeled cells are tdTom-positive, but that a significant part of these do not express the mGFP reporter. In contrast, there are only few cells that are mGFP-positive and tdTom-negative. These data suggest that the *Rosa26*^{tdTom} allele is more sensitive to Cre recombination and raise the possibility that Cre levels might not be saturating in the analyzed tissues, leading to a possible underestimation of the number of the derivatives of Cre-positive cells.

In conclusion, our data indicate that the *Prss56*^{Cre} allele allows specific tracing of adult NSCs and their derivatives in the DG and the SVZ and that quantification of labeled cells must take into account the used reporter allele.

Prss56^{Cre}-traced cells participate in DG development

In the adult DG, *Prss56*^{Cre}-traced cells include granule neurons, astrocytes and type I NSCs. To investigate the

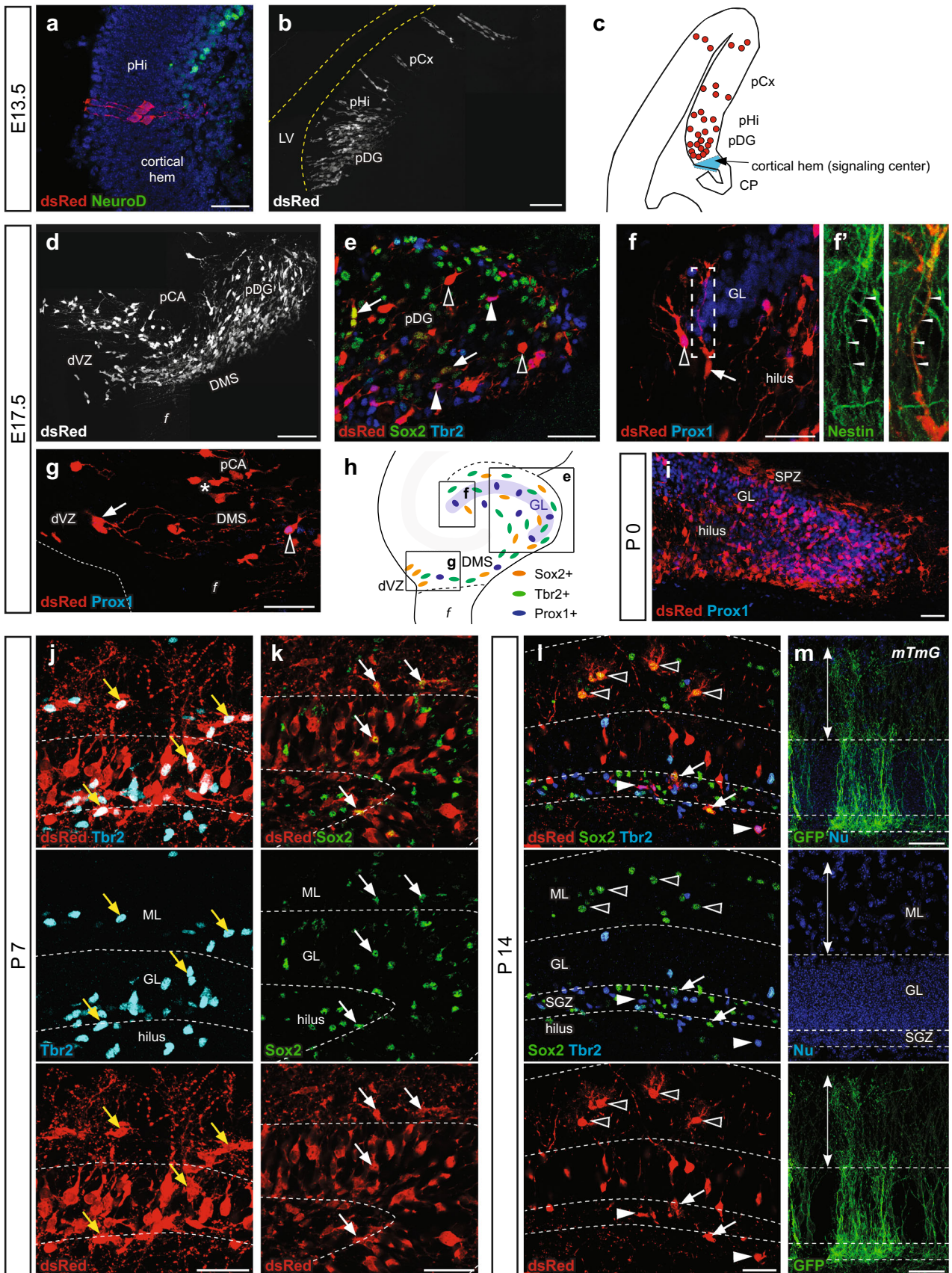
origin of these cells, we followed labeled cells during brain development. The first labeled cells are observed around E13.5 and correspond to radial glia located in the ventricular zone of the prospective DG (Fig. 2a–c). These cells express Nestin and Sox2 (data not shown) and show a radial morphology, with a soma in the ventricular zone and a long process extending to the pial surface (Fig. 2a), indicating that they are radial glia. At this stage, radial glia of the medial pallium are the only reporter-positive cells in the forebrain neuroepithelium (data not shown) and most of them are located near the cortical hem (Fig. 2a–c). These data suggest that *Prss56* activation occurs in the medial pallium around E13.5. As many aspects of the continuous neurogenesis occurring in the DG are still poorly understood (Urbán and Guillemot 2014), we analyzed the participation of reporter-positive radial glia in DG development and the generation of postnatal type I NSCs. At E17.5, reporter-positive cells form a continuous stream extending from the ventricular zone to the prospective DG (Fig. 2d). Most of these cells express markers of radial glia (Nestin and GFAP), neuronal progenitors (Sox2 and Tbr2) and/or immature granule neurons (Prox1) (Fig. 2e–h; Supplemental Fig. 2a, b), indicating that reporter-positive cells contribute to the neuronal lineage (Hodge et al. 2012; Iwano et al. 2012). Near the ventricular zone, reporter-, Prox1-positive cells are often observed in proximity to reporter-, Nestin-positive, radial glial cells (Fig. 2g and data not shown). In the forming DG, reporter-positive Sox2- or Tbr2-positive progenitors are present around and within the prospective granular layer formed by Prox1-positive immature granule neurons and are not segregated in a distinct progenitor layer (Fig. 2e, h). Interestingly, reporter-positive cells expressing Nestin (Fig. 2f, f') or GFAP (Supplemental Fig. 2b) with a soma in the prospective DG might correspond to the so-called secondary radial glia that are believed to generate adult type I NSCs (Brunne et al. 2010). Together, these results suggest that a subpopulation of radial glia in the dentate ventricular zone activates *Prss56* around E13.5 and generates derivatives that migrate toward the DG, where they give rise to local stem cells, progenitors and immature granule neurons (Fig. 2h).

After birth, reporter-positive cells are found in three distinct layers of the developing DG: the hilus, the granular layer, and the subpial zone, which will give rise to the molecular layer in the adult DG (Fig. 2i) (Li et al. 2009). At postnatal day (P) 7, reporter-positive Sox2- and Tbr2-positive progenitors persist in those three layers (Fig. 2j, k; Supplemental Fig. 2c, d) and reporter-positive cells showing a radial morphology and expressing GFAP are observed in the DG (Supplemental Fig. 2c, e). At P14, reporter-positive cells have undergone important morphological and molecular changes: Sox2-positive cells in the

Fig. 2 Derivatives of *Prss56*-expressing cells participate in DG development. **a, b** Coronal confocal optical slice (**a**) and thick section (**b**) through an E13.5 *Prss56^{Cre/+}, Rosa26^{tdTom/+}* medial pallium, showing tdTom-positive cells localized in the prospective DG (pDG), close to the cortical hem identified by the absence of NeuroD in **a**. **c** Schematic representation of the distribution of tdTom-positive cells in the developing pallium. **d–g** Coronal confocal images from different regions of an E17.5 *Prss56^{Cre/+}, Rosa26^{tdTom/+}* prospective DG, showing a stream of tdTom-positive cells extending from the dentate ventricular zone (dVZ) to the pDG in **d**. tdTom-positive cells in the pDG express the progenitor markers Sox2 (**e**, arrows) or Tbr2 (**e**, arrowheads), or the immature granule neuron marker Prox1 (**f**, empty arrowhead). Tbr2- and Sox2-negative, tdTom-positive cells in **e** are indicated by empty arrowheads. Some of the tdTom-positive cells in the pDG retain radial glia morphology (**f**, arrow) and express Nestin (**f**, arrowheads). In **g**, in addition to radial cells (arrow), Prox1-positive, tdTom-labeled immature granule neurons are observed near the dVZ (empty arrowhead), and Prox1-negative tdTom-positive cells are found in the presumptive territory of CA3 (asterisk). **h** Schematic representation of the expression patterns of reporter-positive cells during the formation of the DG. Insets indicate the positions of the pictures in e–g. **i–k** Coronal confocal images of *Prss56^{Cre/+}, Rosa26^{tdTom/+}* P0 (**i**) and P7 (**j**, **k**) DGs showing numerous tdTom-positive cells in the hilus, granular layer and subpial zone. The latter will give rise to the molecular layer. The different layers are delimited by dotted lines. Note that tdTom-, Tbr2-positive (**j**, arrows) and tdTom-, Sox2-positive (**k**, arrows) progenitors are present in all layers at P7. **l** Coronal optical slice of a *Prss56^{Cre/+}, Rosa26^{tdTom/+}* P14 DG showing tdTom-, Sox2-positive cells in the molecular layer, with astrocyte-like bushy morphology (empty arrowheads). In the granular layer, most tdTom-positive cells are Sox2- and Tbr2-negative and have a bright circular soma characteristic of granule neurons. TdTom-, Sox2-positive (arrows) and tdTom-, Tbr2-positive (arrowheads) progenitors are mainly restricted to the hilus and the forming SGZ. **m** Coronal confocal image of a *Prss56^{Cre/+}, Rosa26^{mTmG/+}* P14 DG showing the presence of mGFP-positive radial glia-like type I NSCs, with a soma located in the SGZ and cytoplasmic extensions crossing the granular layer toward the pial surface of the molecular layer (double arrow). CP choroid plexus, DMS dentate migratory stream, dVZ dentate ventricular zone, f fimbria, GL granular layer, ML molecular layer, pCA prospective territory of CA3 fields, pCx prospective cortex, pDG prospective dentate gyrus, pHi prospective territory of the hippocampus, SGZ subgranular zone, SPZ subpial zone. Scale bars 100 μm (**b**, **d**) and 40 μm (others)

molecular layer adopt the “bushy shape” characteristic of astrocytes (Fig. 2l; Supplemental Fig. 2g). Reporter-positive cells in the granular layer mainly correspond to mature neurons (Fig. 2l). Tbr2-, Sox2-, reporter-positive progenitors are mostly restricted to the forming SGZ and hilus (Fig. 2l). Finally, GFAP-positive, adult-like NSCs have established their soma in the SGZ and send radial extensions more apically into the molecular layer than their adult counterpart, suggesting that they have not yet completely matured (Fig. 2m; Supplemental Fig. 2f, h).

A recent study has revealed that NSCs in the DG are spatially heterogeneous and might have different origins during embryogenesis (Li et al. 2013). We therefore analysed the distribution of the cells generated by *Prss56*-expressing radial glia in the adult DG. With both reporting



lines, labeled granule neurons show a dorsal–ventral asymmetry, with a higher concentration in the dorsal DG (Supplemental Fig. 2i–l). This correlates with the distribution of reporter-positive type I NSCs, which are mostly found in the dorsal DG (Supplemental Fig. 2l, 231 ± 65 cells in the dorsal DG vs. 27 ± 12 cells in the ventral DG, $n = 3$). However, a similarly biased distribution was not observed for labeled astrocytes in the DG and oligodendrocytes in the fimbria, the white matter structure linked to the DG (Supplemental Fig. 2j, k, m, n and data not shown). These data suggest that reporter-positive cells are less prone to generate neurogenic stem cells in the ventral DG during development.

Finally, we investigated the fate of reporter-positive radial glia observed in the embryonic hippocampus and cortex (Fig. 2b, c). During development (Supplemental Fig. 2o) and in the adult (Supplemental Fig. 2p–s) the only reporter-positive cells present in the cortex and CA fields are organized in columns and are composed of different combinations of cell types (Supplemental Fig. 2r, s). This result is consistent with a recent description of the pluripotency of clonal radial glia in the cortex (Guo et al. 2013). These reporter-positive cortical columns are most often observed in the areas close to the hippocampus during development and are not likely to derive from adult NSCs but rather from embryonic radial glia.

In conclusion, this analysis indicates that the *Prss56* gene is expressed in a subpopulation of radial glia around E13.5 in the dentate ventricular zone. The pattern of migration and differentiation of their derivatives faithfully recapitulates the successive steps of morphogenesis and neurogenesis of the DG, indicating that these cells participate in its formation, although with an asymmetric final distribution. Our tracing system therefore allows the following of GFAP-positive radial stem cells from E13.5 to the adult stage.

Neural stem cells express *Prss56* in the postnatal ventral SVZ

During embryogenesis, radial glia are the major source of neurons and glia in the developing brain. After birth, the remnants of radial glia lining the lateral ventricle undergo profound morphological and molecular changes, giving rise progressively to ependymal and adult B1 stem cells between P6 and P15 (Tramontin et al. 2003; Merkle et al. 2004; Spassky et al. 2005). We investigated whether, as in the adult DG, reporter-positive adult B1 NSCs are derived from embryonic *Prss56*-expressing radial glia or whether *Prss56* activation occurs postnatally.

Using in situ hybridization, *Prss56* expression was not detected in the lateral wall of lateral ventricles at embryonic or postnatal stages before P7. From P7, it increased to

reach relatively high levels at P14 and P30. This expression was maintained in adulthood at least up to 6 months, although at reduced levels (Fig. 3a). No signal was observed in the *Prss56*^{Cre/Cre} mutant (Fig. 3a). In agreement with these observations, no labeled radial glia was found during embryogenesis or perinatally in *Prss56*^{Cre/+}, *Rosa26*^{tdTom/+} mice. At P2, a few tdTom-positive neuroblasts were observed migrating through the lateral wall and the RMS (Fig. 3b and data not shown) and settling in the OB (Supplemental Fig. 3a). tdTom-positive cells displaying the radial morphology of B1 cells contacting the lateral ventricle were reproducibly observed only from P7 in the ventral lateral wall (Fig. 3c). At P14, larger numbers of tdTom-positive B1 cells are present in the ventral and medial lateral wall of the lateral ventricles (Fig. 3d, e), as well as chains of migrating, tdTom-, DCX-positive neuroblasts (data not shown). From P30, tdTom-positive cells are observed along the entire extent of the lateral wall of the lateral ventricles, in the RMS and the OB (Figs. 1b, 3f).

Prss56 mRNA and reporter-positive B1 cells appear simultaneously in the lateral wall at around P7, indicating that the newly formed B1 cells are those that activate the gene. Furthermore, absence of detection of the mRNA in the dorsal wall, the RMS and the core of the OB (Supplemental Fig. 3b and data not shown) suggests that the gene is not expressed in neuroblasts, nor in interneurons. *Prss56* expression is therefore restricted to B1 cells and eventually to their direct progeny in the SVZ (i.e. in intermediate progenitors). Although tdTom-positive B1 cells express Nestin and GFAP at adult stage (Fig. 1i, j), at P14 tdTom-positive cells with B1 morphology express Nestin, but no GFAP (Fig. 3d–e'). Ependymal cells are not labeled (Fig. 3g). Taken together our data indicate that *Prss56* gene activation in the SVZ is concomitant with the postnatal transformation of radial glia into adult B1 NSCs, prior to the activation of the adult B1 marker GFAP.

During postnatal development, only a few labeled cells are observed in the dorsal part of the lateral wall and none in the dorsal wall of the ventricle (data not shown). The *Prss56* expression pattern shows a similar ventral and medial distribution (Fig. 3a). We investigated whether this situation was maintained in adulthood. We found that *Prss56* was expressed in the adult lateral ventricle along the anterior–posterior axis, but was essentially excluded from the dorsal part of the lateral wall and the dorsal wall (Supplemental Fig. 3b). We studied the distribution of labeled (tdTom-positive) B1 cells in whole-mount preparations of adult lateral wall (Fig. 3g), using labeling of ciliary basal bodies and cell membranes at the apical surface to identify B1 cells, as described previously (Mirzadeh et al. 2008). We measured the distribution of tdTom-positive apical surfaces within six subregions (Fig. 3h). We found differences with the general distribution of B1 cells

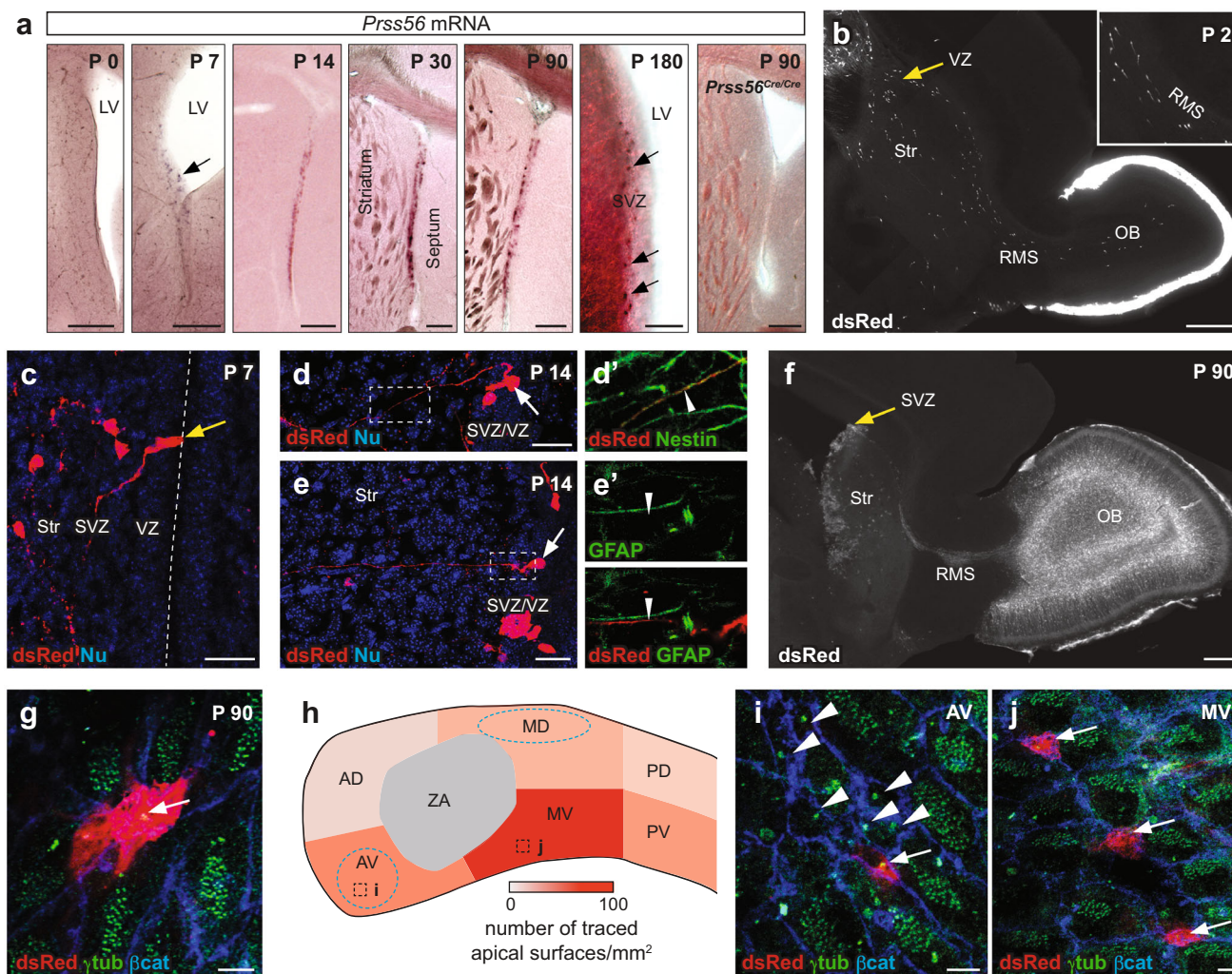


Fig. 3 *Prss56* expression in postnatal NSCs in the ventral SVZ. **a** Detection of *Prss56* mRNA (arrows) by in situ hybridization on coronal slices of wild type and *Prss56*^{Cre/Cre} brains at the indicated stages. **b** Parasagittal section of a *Prss56*^{Cre/+}, *Rosa26*^{tdTom/+} P2 brain, showing the first tdTom-positive cells migrating from the SVZ through the RMS toward the OB. The inset shows a magnification of the RMS. Note that labeled olfactory ensheathing cells are already present in the external part of the OB. **c** Coronal section through the ventral part of a *Prss56*^{Cre/+}, *Rosa26*^{tdTom/+} P7 lateral ventricle showing a tdTom-positive radial B1-like cell contacting the ventricle (arrow). The ventricular surface is indicated by the dotted line. **d–e'** Coronal sections of a *Prss56*^{Cre/+}, *Rosa26*^{tdTom/+} P14 brain showing tdTom-, Nestin-positive (**d'**, arrowhead), GFAP-negative (**e'**), B1-like cells (**d**, **e** arrows). The areas magnified in **d'** and **e'** are indicated in **d** and **e**, respectively. **f** Parasagittal slice of an adult *Prss56*^{Cre/+}, *Rosa26*^{tdTom/+} P90 brain, showing tdTom-positive cells in the SVZ (arrow), RMS and OB. **g** Whole mount preparation of an adult *Prss56*^{Cre/+}, *Rosa26*^{tdTom/+} lateral wall, showing the apical surfaces of tdTom-positive B1 NSCs on an optical slice of a confocal z-stack at the level of the ventricular surface. Note the pinwheel structure

(Mirzadeh et al. 2008): tdTom-positive B1 cells were most abundant in a medial-ventral region (91.8 ± 66.5 tdTom-positive apical surface/mm², $n = 3$; Fig. 3h, j), whereas anterior-ventral and median-dorsal regions, known to be

delineated by the membrane marker β -catenin and the presence of a single basal body marked by γ -tubulin (arrow). Ependymal cells are identified by the presence of multiple basal bodies and by their larger apical surface. **h** Schematic representation of the density of tdTom-positive B1 NSC apical surfaces in six regions of the lateral wall, indicated by red color intensity. The hot spots of B1 NSC apical surface density described by Mirzadeh et al. (2008) are indicated by the blue dotted ellipses. The positions of **i** and **j** are indicated. Regions: AD anterior-dorsal, AV anterior-ventral, MD medial-dorsal, MV medial-ventral, PD posterior-dorsal, PV posterior-ventral, ZA zone of adhesion (between lateral and median walls). **i** Representative optical slice from the anterior-ventral (AV) region of the lateral wall showing a single tdTom-positive B1 NSC apical surface (arrow) in a pinwheel containing 6 tdTom-negative B1 NSC apical surfaces (arrowheads). **j** Representative optical slice from the medial-ventral (MV) region showing 3 isolated, tdTom-positive B1 NSCs' apical surfaces (arrows). *hipp* hippocampus, *LV* lateral ventricle, *OB* olfactory bulb, *RMS* rostral migratory stream, *Str* striatum, *SVZ* subventricular zone, *VZ* ventricular zone. Scale bars 400 μ m (**b**, **f**), 200 μ m (**a**, except P180, 100 μ m), 30 μ m (**c–e**) and 5 μ m (**g**, **i**, **j**)

enriched in B1 cells, showed lower levels of tdTom-positive B1 cells (56.5 ± 39.1 and 35.6 ± 28.2 tdTom-positive apical surface/mm², $n = 3$; Fig. 3h, i). A similar bias was observed in the dorsal–ventral distribution of BrdU-labeled

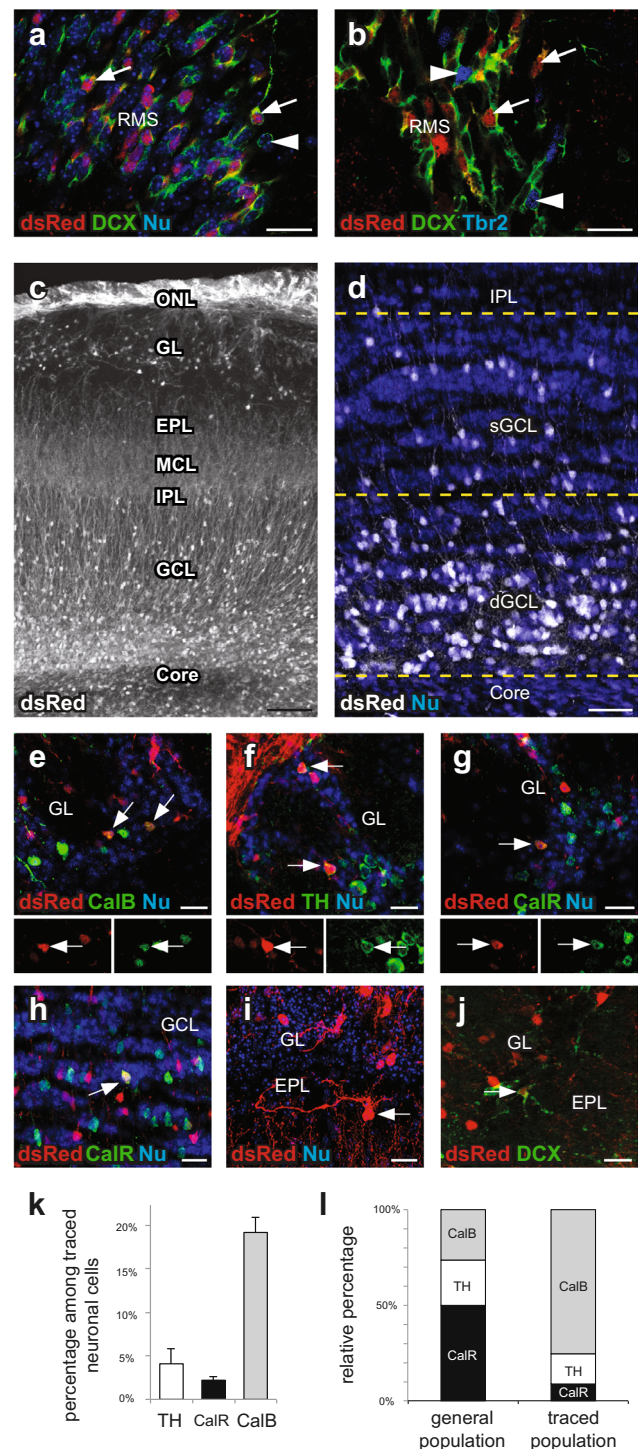
tdTom-positive cells that stay in the SVZ over a three months period and are likely to correspond to B1 cells (Supplemental Fig. 3c). Together, these data indicate that *Prss56* is preferentially expressed in a ventral subpopulation of stem cells in the postnatal SVZ.

Finally, to evaluate the robustness of our system for the analysis of neurogenesis regulation, in particular in view of the non-homogeneous distribution of reporter-positive cells within the SVZ, we evaluated the response of reporter-positive cells to a neurogenic stimulus. For this purpose, we studied the effect of an intracerebroventricular infusion of FGF, a known mitotic agent in the SVZ that stimulates neurogenesis (Jin et al. 2003; Kuhn et al. 1997). We observed that the increase in the number of BrdU-labeled cells was accompanied by an increase in reporter-positive BrdU-positive cells (Supplemental Fig. 3d). These data suggest that the *Prss56^{Cre}* reporter system may constitute an appropriate tool for studying the regulation of neurogenesis in the SVZ.

Prss56^{Cre}-traced SVZ stem cells give rise to deep GC and CalB-positive PGC in the adult OB

Several studies have shown that the fate and localization of newborn interneurons in the mouse OB are determined by the position of their progenitor B1 stem cells in the lateral wall (Stenman et al. 2003; Kohwi et al. 2007; Merkle et al. 2007; Young et al. 2007; Brill et al. 2009; Merkle et al. 2014). For instance, ventral B1 cells generate mainly CalB-positive PGCs and deep GCs, whereas dorsal B1 cells generate mainly tyrosine-hydroxylase (TH)-positive PGCs and superficial GCs, as well as some glutamatergic juxtglomerular neurons (Merkle et al. 2007; Brill et al. 2009). Since we have shown that traced B1 cells are unevenly distributed in the SVZ, we examined their derivatives in the adult RMS and OB.

We first analyzed reporter-positive RMS neuroblasts. In coronal sections through the RMS from 3 month-old *Prss56^{Cre/+}, Rosa26^{tdTom/+}* animals, $22.6 \pm 2.7\%$ ($n = 3$) of the DCX-positive cells were tdTom-positive (Fig. 4a), indicating that tdTom-positive B1 cells significantly contribute to the neurogenic activity of the SVZ niche. No significant difference was observed at different positions along the RMS (data not shown). A proportion of the neuroblasts generated in the dorsal SVZ are known to express the transcription factor *Tbr2* and to differentiate into glutamatergic juxtglomerular neurons (Brill et al. 2009). We detected almost no *Tbr2*-, tdTom-positive neuroblasts in the RMS (only one cluster of 7 tdTom-positive neuroblasts among 915 *Tbr2*-, DCX-positive cells, $n = 3$; Fig. 4b), suggesting that reporter-positive B1 cells do not participate in the generation of glutamatergic neurons.



In the OB granule cell layer, the majority of reporter-positive neurons corresponded to deep GCs (Fig. 4c, d), but some superficial Calretinin (CalR)-positive and -negative GCs were also observed (Fig. 4d, h). In the glomerular layer, the proportions of reporter-positive cells with a neuronal morphology and expressing TH, CalB or CalR (Fig. 4e–g) were determined, revealing a much higher

Fig. 4 Fate of the derivatives of *Prss56*-expressing SVZ B1 NSCs. All analyses were performed in adults. **a** Coronal optical slice at the level of the RMS showing tdTom-positive (*arrows*) and tdTom-negative (*arrowhead*) DCX-positive neuroblasts. **b** Coronal optical slice at the level of the RMS showing that tdTom-, DCX-positive neuroblasts (*arrows*) do not express *Tbr2*. *Tbr2*-positive neuroblasts are indicated by *arrowheads*. **c** Coronal section through the OB showing the presence of numerous tdTom-positive neurons in the GCL, EPL and GL and a dense layer of tdTom-positive olfactory ensheathing cells in the olfactory nerve layer. Note that although neuroblasts are also present in the core of the OB, they are not visible on these images because their fluorescent level is much weaker than that of the neurons. **d** Confocal image at the level of the GCL, showing a higher proportion of tdTom-positive GCs in the deep GCL than the superficial GCL (separated by a *yellow dotted line*). **e–g** Confocal optical slices showing tdTom-positive PGCs, also positive for CalB (**e**, *arrows*), TH (**f**, *arrows*) and CalR (**g**, *arrow*). Separated channels are shown below. **h** Optical slice showing a tdTom-, CalR-positive superficial GC (*arrow*). **i** Confocal image showing a tdTom-positive cell in the external plexiform layer with a morphology similar to the recently described type-4 subtype (*arrow*). **j** Confocal image showing a tdTom-, DCX-positive cell in the GL (*arrow*). **k, l** Quantitative analysis of the distribution of the tdTom-positive PGC population. Only round-shaped tdTom-positive cells in the GL were considered as tdTom-positive PGCs. The percentage of CalB-, TH- and CalR-positive cells among tdTom-positive PGCs is shown in **k** and their relative proportions are compared to those of the general population (Kohwi et al. 2007) in **l**. *EPL* external plexiform layer, *GCL* granule cell layer, *GL* glomerular layer, *IPL* internal plexiform layer, *MCL* mitral cell layer, *ONL* olfactory nerve layer, *RMS* rostral migratory stream, *dGCL* deep GCL, *sGCL* superficial GCL. *Scale bars* 150 μm (**c**), 40 μm (**d**) and 20 μm (**a, b, e–j**)

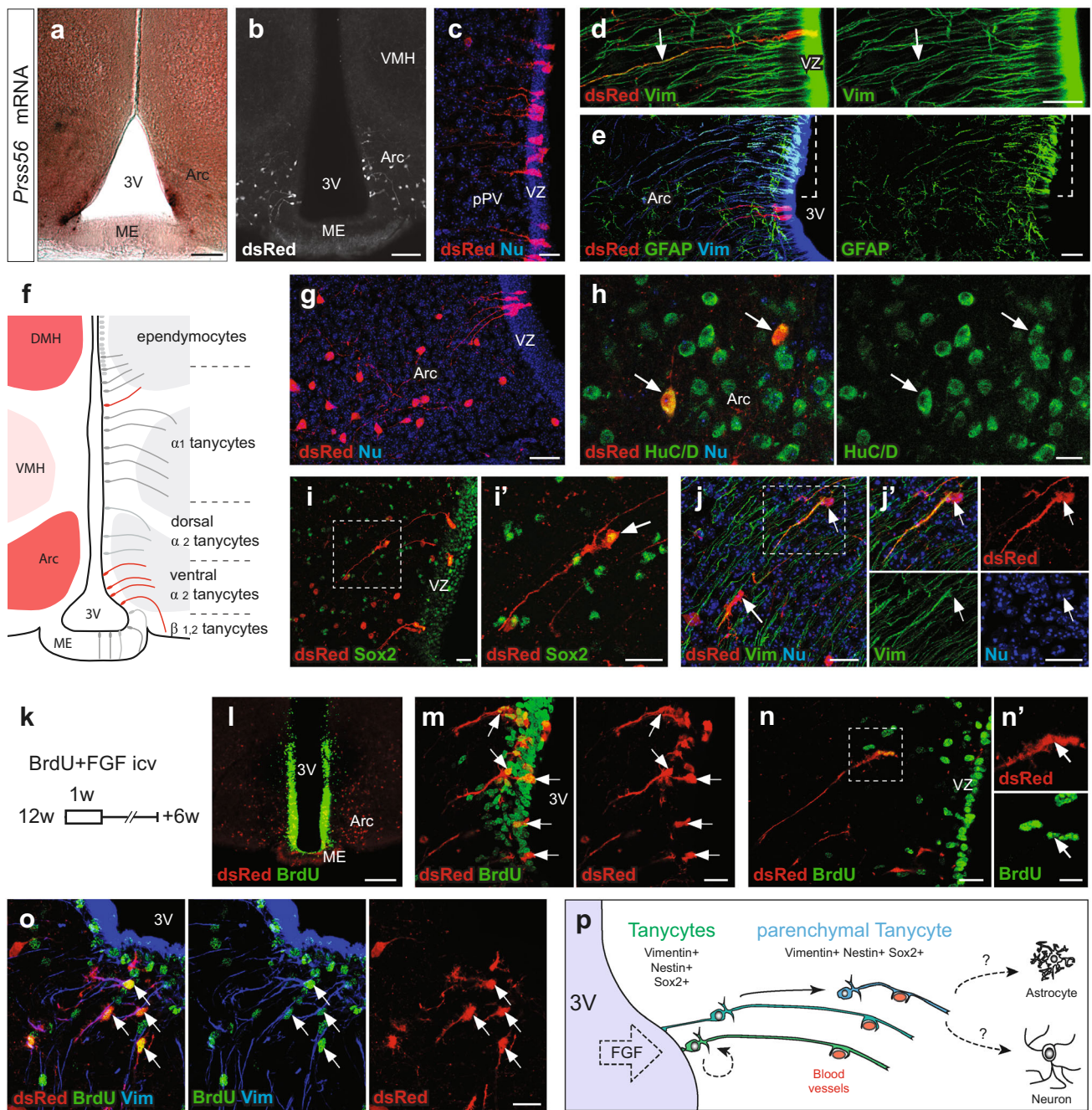
proportion of CalB-positive neurons ($19.8 \pm 4.8\%$) than TH-positive ($4.0 \pm 4.3\%$) or CalR-positive neurons ($2.2 \pm 1.7\%$), in contrast to the general neuronal distribution ($n = 4$, Fig. 4k, l). This analysis also revealed that most (75 %) of the dTom-positive PGCs did not express any of the three markers. Accordingly, it has previously been shown, with tracing based on the expression of *Dlx1/2* in the ventral SVZ, that many periglomerular interneurons are not positive for any of these markers (Batista-Brito et al. 2008). A few reporter-positive neurons were also observed at the level of the external plexiform layer and had a morphology similar to the recently described type 4 cells (Fig. 4i; Merkle et al. 2014). Finally, reporter-, DCX-positive neuroblasts were observed in different layers and represented approximately 6 % of the reporter-positive neuronal progeny in the glomerular layer (Fig. 4j). In conclusion, these data indicate that reporter-positive B1 cells generate a large variety of neuronal populations, present in the different layers of the OB after birth. This neurogenic potential is nevertheless restricted and reflects the medial-ventral localization of reporter-positive B1 cells in the SVZ.

In the OB, *Prss56*^{Cre}-traced cells were also observed in the olfactory nerve layer and correspond to olfactory ensheathing cells (Figs. 1b, 3b, f; Supplemental Fig. 3a). As revealed by in situ hybridization, *Prss56* expression is

initiated in the olfactory nerve layer at around E13.5 and persists in the adult (Supplemental Fig. 4a–c'). Comparison with the SVZ indicated higher relative levels of expression in the olfactory nerve layer (data not shown). Accordingly, most labeled olfactory ensheathing cells are positive for both reporters in *Prss56*^{Cre/+}, *Rosa26*^{tdTom/mTmG} mice (Supplemental Fig. 1f), suggesting that the Cre level is not limiting for the recombination in these cells and that recombination efficiency is correlated with the level of *Prss56* expression. Olfactory ensheathing cells are a heterogeneous population of cells, with a subpopulation derived from the neural crest and expressing *Sox10* (Barraud et al. 2010; Forni et al. 2011). Traced olfactory ensheathing cells were found to express *Sox10* from E13.5 to adulthood (Supplemental Fig. 4d–f). They are restricted to the inner olfactory nerve layer (Supplemental Fig. 4f, g) and absent from the olfactory nerve (Supplemental Fig. 4a, d, d'). In the adult, they are positive for BLBP, but not GFAP (Supplemental Fig. 4f–g'). These results indicate that *Prss56* constitutes a marker for an olfactory ensheathing cells subpopulation in the central nervous system.

***Prss56* is expressed in a subpopulation of tanycytes in the adult hypothalamus**

Emerging evidence indicates that new neurons are generated in the adult hypothalamus, suggesting the existence of a local neurogenic niche (Robins et al. 2013a). As *Prss56* is expressed in two other neurogenic niches, we investigated the transcription of *Prss56* in the adult hypothalamus by in situ hybridization. We found that the gene is expressed in the ventricular region of the third ventricle, at the level of the arcuate nucleus (Fig. 5a; Supplemental Fig. 5a, b). Tracing of *Prss56*-expressing cells revealed labeled cells in the same region of the postnatal and adult hypothalamus (Fig. 5b, c; Supplemental Fig. 5c). The reporter-positive cells correspond to tanycytes: they line the ventricular wall of the ventral third ventricle, express tanycyte markers like Vimentin (Fig. 5d, e) and Nestin (Supplemental Fig. 5d) and send a single radial extension toward the parenchyma, often contacting blood vessels (Fig. 5b–e and data not shown). These reporter-positive tanycytes are located in a specific region, extending from the anterior part of the arcuate nucleus to the posterior part of the periventricular nucleus, below the median mammillary nucleus (Supplemental Fig. 5e, e'). Consistent with *Prss56* mRNA localization, no reporter-positive tanycytes were observed in the medial eminence or the ventromedial nucleus, and only a few were found scattered in the dorsomedial nucleus (Fig. 5b; Supplemental Fig. 5e, e'). The localization of most of the labeled tanycytes suggests that they belong to the $\alpha 2$ subtype (Fig. 5f). Previous studies have shown that



GFAP is only expressed in dorsal $\alpha 2$ and a fraction of $\alpha 1$ tanyocytes (Haan et al. 2013; Robins et al. 2013a). At the level of the arcuate nucleus, reporter-positive tanyocytes are located just below the GFAP-positive tanyocyte population, but they never express this marker (Fig. 5e; Supplemental Fig. 5c). In the adult *Prss56*^{Cre/+}, *Rosa26*^{tdTom/+} brain, the tdTom-positive tanyocytes (421 ± 104 cells per hypothalamus, $n = 3$) represent only a small proportion of the

Vimentin-positive tanyocytes (Fig. 5d, e). Together, these results indicate that *Prss56*-expressing cells in the hypothalamus belong to a ventral, GFAP-negative subpopulation of $\alpha 2$ tanyocytes (Fig. 5f).

Consistent with the distribution of the reporter-positive tanyocytes, many tdTom-, HuC/D-positive neuronal cells were observed in the postnatal arcuate and dorsomedial nuclei, whereas the medial eminence and the ventromedial

Fig. 5 *Prss56* is expressed in a subpopulation of tanycytes in the adult hypothalamus. **a** Detection of *Prss56* mRNA by in situ hybridization in a coronal slice of adult hypothalamus showing *Prss56* expression in the ventricular zone at the level of the arcuate nucleus. **b** Coronal slice of adult *Prss56*^{Cre/+}, *Rosa26*^{tdTom/+} brain showing tdTom-positive cells in the arcuate nucleus, but not in the median eminence and the ventromedial nucleus of the hypothalamus. **c** Confocal image of an adult *Prss56*^{Cre/+}, *Rosa26*^{tdTom/+} brain at the level of the periventricular nucleus showing tdTom-positive tanycytes with a soma lining the third ventricle and radial morphology. **d** Confocal image of an adult *Prss56*^{Cre/+}, *Rosa26*^{tdTom/+} brain, showing tdTom-positive tanycytes that express Vimentin (arrow). **e** Optical confocal slice of an adult *Prss56*^{Cre/+}, *Rosa26*^{tdTom/+} brain at the level of the arcuate nucleus showing that tdTom-positive tanycytes do not express GFAP and are localized ventrally to the GFAP-positive region indicated by the dotted line. **f** Schematic representation of the distribution of tdTom-positive tanycytes (on the right) along the ventricle and tdTom-positive neurons within the nuclei of the mediobasal hypothalamus (red nuclei on the left). **g**, **h** Confocal image of an adult *Prss56*^{Cre/+}, *Rosa26*^{tdTom/+} brain showing numerous tdTom-positive neurons in the arcuate nucleus that are positive for the neuronal marker HuC/D (arrows in **h**). **i**, **i'** Optical slice of an adult *Prss56*^{Cre/+}, *Rosa26*^{tdTom/+} brain showing a tdTom-, Sox2-positive tanycyte-like cell (**i'**, arrow) with a cell body in the parenchyma, outside of the ventricular zone (VZ in **i**). **j**, **j'** Confocal stack from an adult *Prss56*^{Cre/+}, *Rosa26*^{tdTom/+} brain showing two tdTom-, Vimentin-positive parenchymal tanycyte-like cells (arrows). Note the common direction of the extensions of the tdTom-positive parenchymal tanycyte-like cells with the Vimentin-positive extensions of the ventricular tanycytes. **k–o** BrdU labeling of proliferating hypothalamus cells. BrdU and FGF-2 were infused in the ventricular system of adult *Prss56*^{Cre/+}, *Rosa26*^{tdTom/+} animals for 7 days and tissues were harvested 6 weeks later as illustrated in **k**. **l** Coronal slice at the level of the arcuate nucleus showing tracing (red) and BrdU labeling (green). **m** Confocal image showing a high number of BrdU-positive nuclei, including those of tdTom-positive tanycytes, in the thickened VZ due to FGF mitogen exposure. **n**, **o** Confocal images showing tdTom-, BrdU-positive (arrows in **n**), and also Vimentin-positive (**o**) parenchymal tanycyte-like cells. **p** Schematic representation of the generation of parenchymal tanycyte-like cells by nuclear translocation of ventricular tanycytes. 3V third ventricle, Arc arcuate nucleus, DMH dorsomedial nucleus, icv intracerebroventricular infusion, ME median eminence, pPV posterior part of the periventricular nucleus, VMH ventromedial nucleus, VZ ventricular zone. Scale bars 200 μ m (**l**), 100 μ m (**a**, **b**), 40 μ m (**g**), 20 μ m (**c–e**, **h–j'**, **m–o**) and 10 μ m (**n'**)

nucleus were mostly free of labeled cells (Fig. 5b, f–h; Supplemental Fig. 5e). In addition, a few Sox2-positive astrocytes were also labeled in the same areas (less than 10 astrocytes per mediobasal hypothalamus, $n = 5$; data not shown). We did not observe reporter-positive cells also positive for NG2, a potential marker of stem cells in the parenchyma (Robins et al. 2013b). These data suggest that *Prss56*^{Cre}-traced $\alpha 2$ tanycytes could generate reporter-positive neurons observed in the arcuate and dorsomedial nuclei after birth. In the parenchyma, we also observed reporter-positive cells that had the elongated morphology of tanycytes, but with a cell body located 60–100 μ m away from the ventricular surface and an extension perpendicular to this surface (Fig. 5 i–j'). These cells are positive for the tanycyte markers Sox2, Vimentin and Nestin (Fig. 5i–j';

Supplemental Fig. 5d). To our knowledge, this parenchymal tanycyte-like population has not been previously described and may correspond to ventricular tanycytes that have translocated their soma into the parenchyma. To determine whether reporter-positive adult tanycytes proliferate and can indeed generate these parenchymal tanycyte-like cells, BrdU and FGF2 were infused in the brain of 3 month-old *Prss56*^{Cre/+}, *Rosa26*^{tdTom/+} mice, as FGF2 has been reported to stimulate proliferation of tanycytes (Robins et al. 2013a). Six weeks after infusion (Fig. 5k), we observed numerous BrdU-positive cells in the third ventricular wall, especially at the level of the arcuate nucleus (Fig. 5l). tdTom-positive tanycytes efficiently incorporated BrdU (Fig. 5m). We also observed BrdU-, tdTom-positive cells corresponding to the parenchymal tanycyte-like population, as well as tanycyte-like cells with intermediate positions between the latter and the ventricular surface (Fig. 5m–o; Supplemental Fig. 5f, f'). We verified that, under such mitogenic stimulation, the parenchymal BrdU-positive tanycyte-like cells express Vimentin, Nestin and Sox2, and do not express GFAP, NG2 or DCX (Fig. 5o; Supplemental Fig. 5 g–j and data not shown). Taken together, our data suggest that the $\alpha 2$ tanycytes are able to migrate into the parenchyma, in physiological conditions and upon mitogenic stimulation.

Discussion

Since the pioneering experiments of Ezra Allen (Allen 1912) and Joseph Altman (Altman and Das 1965a, b), adult neurogenesis has been recognized as a natural process in the brain. Although it provides only a small fraction of new neurons in specific regions of the brain, these neurons are necessary for many physiological brain functions, such as learning, memory and mood regulation (Zhao et al. 2008). Because it concerns only very limited cell populations, embedded in complex niches, the study of adult neurogenesis has heavily relied on specific labeling procedures (Enikolopov et al. 2015). In this report, we describe a novel tracing system, based on a *Prss56*^{Cre} allele, which allows the identification of NSCs and their derivatives in three neurogenic niches of the adult brain. This system, as well as additional genetic constructions based on the *Prss56* locus, should constitute useful tools to investigate multiple aspects of adult neurogenesis in the mouse.

Within each niche, NSCs have been reported to show regional variations, reflecting different embryonic origins and related to different neuronal fates (Stenman et al. 2003; Kohwi et al. 2007; Merkle et al. 2007; Young et al. 2007; Brill et al. 2009; Merkle et al. 2014). The *Prss56*^{Cre}-based tracing system works in several niches, but only a subset of NSCs is labeled within each niche, possibly reflecting

regional variations. This restricted tracing might therefore constitute an advantage for the identification, isolation, and fate analysis of specific NSC populations. Although the proportion of reporter-positive cells may underestimate the number of *Prss56*-positive cells, this should not affect our conclusions on regional variations, as the efficiency of reporter recombination is correlated with the level of *Prss56* expression. Our tracing system also revealed dramatic differences in the timing of *Prss56* activation between the different niches. In the hippocampus, reporter expression is first observed in a small group of radial glial cells in the medial pallium at embryonic day 13.5. These cells are most likely the progenitors of the reporter-positive adult NSCs observed in the DG after P14. In contrast, in the SVZ, the *Prss56* gene is only activated when the radial glia are transformed into B1 NSCs, in the second week after birth and remains expressed during adulthood. These differences are likely to reflect specificities in the regulation and function of *Prss56* in the different niches.

The present study also revealed major differences in the behavior of two reporters, *Rosa26^{mTmG}* and *Rosa26^{tdTom}*. The cellular localization of the reporter, membrane-targeted for GFP, and cytoplasmic for tdTom, affects the visualization of NSCs and neurons in opposite manners. In addition, the observed differences may also rely on variations in levels of the expression of the reporters in different cell types. Finally we established that in case of low levels of expression of the Cre recombinase, the *Rosa26^{tdTom}* allele recombines more efficiently than the *Rosa26^{mTmG}* allele. Our data therefore highlight the importance of the choice of the reporter gene in fate mapping studies. This work provides a guide for the most appropriate reporters in studies of NSCs and their derivatives, and argues in favor of testing several reporters in other situations.

According to a classical view, the DG originates from stem/progenitor cells of the medial pallium ventricular zone, which migrate during later stages of embryonic development to the pial side of the median cortex and the hippocampal fissure (Urbán and Guillemot 2014). These cells show astrocytic features, express GFAP and Nestin, and will form the SGZ in the perinatal and postnatal periods (Seri et al. 2001; Fukuda et al. 2003; Liu et al. 2010; Seki et al. 2013). An element of this model is that the adult DG contains a homogenous pool of NSCs that have been generated during embryonic development. Recently, long-term fate mapping studies have shown that, in the perinatal period, cells from the ventral hippocampus respond to Sonic Hedgehog and also migrate to the dorsal region, establishing a pool of NSCs in the adult SGZ (Li et al. 2013). This study suggests that, like the SVZ, the DG is a mosaic structure, with NSCs originating from different embryonic regions (Merkle et al. 2007; Li et al. 2013). Our data are consistent with the classical model, as they

indicate that the labeled adult NSCs are generated from a subpopulation of radial glia of the medial pallium that migrate to the DG in the late embryonic period. However, since only a fraction of the NSCs are reporter-positive and these are more abundant in the dorsal region, our data do not exclude heterogeneity in the pool of adult NSCs in the SGZ. The *Prss56^{Cre}* allele provides the first endogenous system allowing specific tracing of a DG radial glia subpopulation. It should therefore constitute an appropriate tool to ablate genes involved in different aspects of this particular process of neurogenesis (e.g. quiescence, migration, differentiation), without compromising the development of the DG.

In the SVZ, the activation of *Prss56* and the appearance of the first reporter-positive B1 cells occur during the second postnatal week, in parallel with the transformation of radial glial cells into adult NSCs (Tramontin et al. 2003; Merkle et al. 2004). This suggests that, in this territory, expression of *Prss56* is specific to adult NSCs. However, nothing is known about the regulation of this gene. Whereas adult NSCs that generate OB interneurons are present in the different walls of the lateral ventricles and in the RMS (Alonso et al. 2008; Mirzadeh et al. 2008), the expression of *Prss56* is restricted to the ventral and medial regions of the lateral wall, with a pattern similar to that of *Gli1* in the adult (Ihrig et al. 2011). This raises the possibility that *Prss56*, like *Gli1*, may respond to Sonic Hedgehog signaling. Although reporter-positive B1 cells generate a large variety of neuronal populations, present in the different layers of the OB after birth, most of the reporter-positive neurons are deep GCs and CalB-positive PGCs. This is consistent with the higher density of reporter-positive B1 cells in the ventral portion of the lateral wall, which are known to preferentially give rise to these two types of neurons (Merkle et al. 2007).

The discovery of postnatal neurogenesis in the hypothalamus and the involvement of tanycytes in this process is recent (Sousa-Ferreira et al. 2014). The hypothalamus plays important roles in numerous physiological and behavioral functions, and feeding has certainly attracted the greatest attention (Pierce and Xu 2010; Lee and Blackshaw 2012; Li et al. 2012; Sousa-Ferreira et al. 2014). However, the contribution of postnatal neurogenesis to these functions still remains to be established. Such a demonstration and, more generally, the study of neurogenesis in this region are challenging, because tanycytes divide very slowly and it is difficult to perform viral labeling or genetic fate mapping studies that target this specific population. Tracing with *Prss56^{Cre}* has allowed us to label a subpopulation of GFAP-negative $\alpha 2$ tanycytes and neurons of the arcuate nucleus, suggesting that these cells belong to the same lineage. Furthermore, we also observed labeled parenchymal tanycyte-like cells that have

not been previously described. BrdU labeling, combined with FGF infusion, suggests that these parenchymal tanyocyte-like cells are also part of this lineage and derive from the ventricular tanycytes by translocation of their soma into the parenchyma (Fig. 5p). It will be important to determine whether this translocation is a necessary step in the neurogenic/gliogenic process occurring in the adult hypothalamus or whether parenchymal tanycytes constitute a different cell population, with specific functions. Our tracing system should be helpful to investigate this issue and more generally to expand the analysis of neurogenesis in the hypothalamus.

Finally, a number of studies, using various methodological approaches, such as ³H-thymidine autoradiography, BrdU labeling, and neurosphere formation, have reported the presence of new neurons and progenitor cells in multiple brain regions outside of the SGZ, the SVZ, and the hypothalamus. These regions include the basal forebrain (Palmer et al. 1995), the striatum (Reynolds et al. 1992; Pencea et al. 2001), the amygdala (Rivers et al. 2008), the substantia nigra (Lie et al. 2002), and the subcortical white matter (Nunes et al. 2003). However, these observations have been received with skepticism and the question of whether adult neurogenesis exists in these regions remains open (Gould 2007; Lee and Blackshaw 2012). In this report, we have established that the tracing system based on the *Prss56^{Cre}* allele has allowed us to follow adult NSCs and their derivatives in three established neurogenic niches. It is possible that *Prss56* is also expressed in adult NSCs in other potential niches and the *Prss56^{Cre}* allele would therefore also constitute an extremely useful tool to investigate neurogenesis in those niches that are still subject to controversy.

Acknowledgments We are grateful to the IBENS Imaging Facility, which received the support of grants from the “Région Ile-de-France” (NERF No. 2009-44 and NERF No. 2011-45), the “Fondation pour la Recherche Médicale” (No. DGE 20111123023) and the “Fédération pour la Recherche sur le Cerveau—Rotary International France” (2011). The IBENS Imaging Facility also received support implemented by the ANR under the program «Investissements d’Avenir», with the references: ANR-10-LABX-54 MEMO LIFE, ANR-11-IDEX-0001-02 PSL* Research University and ANR-10-INSB-04-01 France-BioImaging infrastructure. We are also grateful to the IBENS mouse facility, in particular A. Boudjouher and C. Auger. We thank Nathalie Rouach and Annette Koulakoff (College de France, France) for the gift of the *hGfAP::GFP* line. The P.C. laboratory was financed by the Institut National de la Recherche Médicale (INSERM), the Centre National de la Recherche Scientifique (CNRS), the Ministère de la Recherche et Technologie (MRT), the Fondation pour la Recherche Médicale (FRM), the Association Française contre les Myopathies (AFM), and the Association de Recherche sur le Cancer (ARC). It has received support under the program “Investissements d’Avenir” launched by the French Government and implemented by the ANR, with the references: ANR-10-LABX-54 MEMOLIFE and ANR-11-IDEX-0001-02 PSL* Research University. A.J. was supported by a doctoral grant from Sorbonne Universités and by the

MEMOLIFE program. A.G. was supported by the Fondation Pierre Gilles de Gennes, FRM (SPF20101221087), MRT and the MEMO-LIFE program.

Compliance with ethical standards

Conflict of interest The authors declare no competing financial interests.

References

- Allen E (1912) The cessation of mitosis in the central nervous system of the albino rat. *J Comp Neurol* 22:547–568
- Alonso M, Ortega-Pérez I, Grubb MS, Bourgeois J-P, Charneau P, Lledo P-M (2008) Turning astrocytes from the rostral migratory stream into neurons: a role for the olfactory sensory organ. *J Neurosci* 28:11089–11102
- Altman J, Das GD (1965a) Autoradiographic and histological evidence of postnatal hippocampal neurogenesis in rats. *J Comp Neurol* 124:319–335
- Altman J, Das GD (1965b) Post-natal origin of microneurons in the rat brain. *Nature* 207:953–956
- Barraud P, Seferiadis AA, Tyson LD, Zwart MF, Szabo-Rogers HL, Ruhrberg C, Liu KJ, Baker CVH (2010) Neural crest origin of olfactory ensheathing glia. *Proc Natl Acad Sci USA* 107:21040–21045
- Batista-Brito R, Close J, Machold R, Fishell G (2008) The distinct temporal origins of olfactory bulb interneuron subtypes. *J Neurosci* 28:3966–3975
- Beckervordersandforth R, Tripathi P, Ninkovic J, Bayam E, Lepier A, Stempfhuber B, Kirchoff F, Hirrlinger J, Haslinger A, Lie DC, Beckers J, Yoder B, Irmeler M, Götz M (2010) In vivo fate mapping and expression analysis reveals molecular hallmarks of prospectively isolated adult neural stem cells. *Cell Stem Cell* 7:744–758
- Brill MS, Ninkovic J, Winpenny E, Hodge RD, Ozen I, Yang R, Lepier A, Gascón S, Erdelyi F, Szabo G, Parras C, Guillemot F, Frotscher M, Berninger B, Hevner RF, Raineteau O, Götz M (2009) Adult generation of glutamatergic olfactory bulb interneurons. *Nat Neurosci* 12:1524–1533
- Brunne B, Zhao S, Derouiche A, Herz J, May P, Frotscher M, Bock HH (2010) Origin, maturation, and astroglial transformation of secondary radial glial cells in the developing dentate gyrus. *Glia* 58:1553–1569
- Couplier F, Le Crom S, Maro GS, Manent J, Giovannini M, Maciorowski Z, Fischer A, Gessler M, Charnay P, Topilko P (2009) Novel features of boundary cap cells revealed by the analysis of newly identified molecular markers. *Glia* 57:1450–1457
- Deshpande A, Bergami M, Ghanem A, Conzelmann K-K, Lepier A, Götz M, Berninger B (2013) Retrograde monosynaptic tracing reveals the temporal evolution of inputs onto new neurons in the adult dentate gyrus and olfactory bulb. *Proc Natl Acad Sci USA* 110:E1152–E1161
- Enikolopov G, Overstreet-Wadiche L, Ge S (2015) Viral and transgenic reporters and genetic analysis of adult neurogenesis. *Cold Spring Harb Perspect Biol* 7:a018804
- Ernst A, Alkass K, Bernard S, Salehpour M, Perl S, Tisdale J, Possnert G, Druid H, Frisén J (2014) Neurogenesis in the striatum of the adult human brain. *Cell* 156:1072–1083
- Espósito MS, Piatti VC, Laplagne DA, Morgenstern NA, Ferrari CC, Pitossi FJ, Schinder AF (2005) Neuronal differentiation in the adult hippocampus recapitulates embryonic development. *J Neurosci* 25:10074–10086

- Forni PE, Taylor-Burds C, Melvin VS, Williams T, Wray S (2011) Neural crest and ectodermal cells intermix in the nasal placode to give rise to GnRH-1 neurons, sensory neurons, and olfactory ensheathing cells. *J Neurosci* 31:6915–6927
- Fukuda S, Kato F, Tozuka Y, Yamaguchi M, Miyamoto Y, Hisatsune T (2003) Two distinct subpopulations of nestin-positive cells in adult mouse dentate gyrus. *J Neurosci* 23:9357–9366
- Gage FH, Temple S (2013) Neural stem cells: generating and regenerating the brain. *Neuron* 80:588–601
- Gal A, Rau I, El Matri L, Kreienkamp H-J, Fehr S, Baklouti K, Chouchane I, Li Y, Rehbein M, Fuchs J, Fledelius HC, Vilhelmsen K, Schorderet DF, Munier FL, Ostergaard E, Thompson DA, Rosenberg T (2011) Autosomal-recessive posterior microphthalmos is caused by mutations in *PRSS56*, a gene encoding a trypsin-like serine protease. *Am J Hum Genet* 88:382–390
- Ge S, Yang C-H, Hsu K-S, Ming G-L, Song H (2007) A critical period for enhanced synaptic plasticity in newly generated neurons of the adult brain. *Neuron* 54:559–566
- Gould E (2007) How widespread is adult neurogenesis in mammals? *Nat Rev Neurosci* 8:481–488
- Gresset A, Couplier F, Gerschenfeld G, Jourdon A, Matesic G, Richard L, Vallat J-M, Charnay P, Topilko P (2015) Boundary caps give rise to neurogenic stem cells and terminal glia in the skin. *Stem Cell Rep* 5:1–13
- Guo C, Eckler MJ, McKenna WL, McKinsey GL, Rubenstein JLR, Chen Bin (2013) Fezf2 expression identifies a multipotent progenitor for neocortical projection neurons, astrocytes, and oligodendrocytes. *Neuron* 80:1167–1174
- Haan N, Goodman T, Najdi-Samiei A, Stratford CM, Rice R, El Agha E, Bellusci S, Hajhosseini MK (2013) Fgf10-expressing tanyocytes add new neurons to the appetite/energy-balance regulating centers of the postnatal and adult hypothalamus. *J Neurosci* 33:6170–6180
- Hodge RD, Nelson BR, Kahoud RJ, Yang R, Mussar KE, Reiner SL, Hevner RF (2012) *Tbr2* is essential for hippocampal lineage progression from neural stem cells to intermediate progenitors and neurons. *J Neurosci* 32:6275–6287
- Ihrig RA, Álvarez-Buylla A (2011) Lake-front property: a unique germinal niche by the lateral ventricles of the adult brain. *Neuron* 70:674–686
- Ihrig RA, Shah JK, Harwell CC, Levine JH, Guinto CD, Lezameta M, Kriegstein AR, Álvarez-Buylla A (2011) Persistent Sonic Hedgehog signaling in adult brain determines neural stem cell positional identity. *Neuron* 71:250–262
- Iwano T, Masuda A, Kiyonari H, Enomoto H, Matsuzaki F (2012) *Prox1* postmitotically defines dentate gyrus cells by specifying granule cell identity over CA3 pyramidal cell fate in the hippocampus. *Development* 139:3051–3062
- Jin K, Sun Y, Xie L, Bateau S, Mao XO, Smelick C, Logvinova A, Greenberg DA (2003) Neurogenesis and aging: FGF-2 and HB-EGF restore neurogenesis in hippocampus and subventricular zone of aged mice. *Aging Cell* 2:175–183
- Kempermann G, Jessberger S, Steiner B, Kronenberg G (2004) Milestones of neuronal development in the adult hippocampus. *Trends Neurosci* 27:447–452
- Kohwi M, Petryniak MA, Long JE, Ekker M, Obata K, Yanagawa Y, Rubenstein JLR, Álvarez-Buylla A (2007) A subpopulation of olfactory bulb GABAergic interneurons is derived from *Emx1*- and *Dlx5/6*-expressing progenitors. *J Neurosci* 27:6878–6891
- Kokoeva MV, Yin H, Flier JS (2005) Neurogenesis in the hypothalamus of adult mice: potential role in energy balance. *Science* 310:679–683
- Kuhn HG, Winkler J, Kempermann G, Thal LJ, Gage FH (1997) Epidermal growth factor and fibroblast growth factor-2 have different effects on neural progenitors in the adult rat brain. *J Neurosci* 17:5820–5829
- Lee DA, Blackshaw S (2012) Functional implications of hypothalamic neurogenesis in the adult mammalian brain. *Int J Dev Neurosci* 30:615–621
- Lee DA, Bedont JL, Pak T, Wang H, Song J, Miranda-Angulo A, Takiar V, Charubhumi V, Balordi F, Takebayashi H, Aja S, Ford E, Fishell G, Blackshaw S (2012) Tanyocytes of the hypothalamic median eminence form a diet-responsive neurogenic niche. *Nat Neurosci* 15:700–702
- Lepousez G, Nissant A, Bryant AK, Gheusi G, Greer CA, Lledo PM (2014) Olfactory learning promotes input-specific synaptic plasticity in adult-born neurons. *Proc Natl Acad Sci USA* 111:13984–13989
- Li G, Kataoka H, Coughlin SR, Pleasure SJ (2009) Identification of a transient subpial neurogenic zone in the developing dentate gyrus and its regulation by *Cxcl12* and *reelin* signaling. *Development* 136:327–335
- Li J, Tang Y, Cai D (2012) *IKKβ/NF-κB* disrupts adult hypothalamic neural stem cells to mediate a neurodegenerative mechanism of dietary obesity and pre-diabetes. *Nat Cell Biol* 14:999–1012
- Li G, Fang L, Fernández G, Pleasure SJ (2013) The ventral hippocampus is the embryonic origin for adult neural stem cells in the dentate gyrus. *Neuron* 78:658–672
- Lie DC, Dziejczapolski G, Willhoite AR, Kaspar BK, Shults CW, Gage FH (2002) The adult substantia nigra contains progenitor cells with neurogenic potential. *J Neurosci* 22:6639–6649
- Liu Y, Namba T, Liu J, Suzuki R, Shioda S, Seki T (2010) Glial fibrillary acidic protein-expressing neural progenitors give rise to immature neurons via early intermediate progenitors expressing both glial fibrillary acidic protein and neuronal markers in the adult hippocampus. *Neuroscience* 166:241–251
- Lois C, Alvarez-Buylla A (1994) Long-distance neuronal migration in the adult mammalian brain. *Science* 264:1145–1148
- Madisen L, Zwingman TA, Sunkin SM, Oh SW, Zariwala HA, Gu H, Ng LL, Palmiter RD, Hawrylycz MJ, Jones AR, Lein ES, Zeng H (2010) A robust and high-throughput Cre reporting and characterization system for the whole mouse brain. *Nat Neurosci* 13:133–140
- Marín-Burgin A, Mongiat LA, Pardi MB, Schinder AF (2012) Unique processing during a period of high excitation/inhibition balance in adult-born neurons. *Science* 335:1238–1242
- Markakis EA, Palmer TD, Randolph-Moore L, Rakic P, Gage FH (2004) Novel neuronal phenotypes from neural progenitor cells. *J Neurosci* 24:2886–2897
- Merkle FT, Tramontin AD, Garcia-Verdugo J-M, Álvarez-Buylla A (2004) Radial glia give rise to adult neural stem cells in the subventricular zone. *Proc Natl Acad Sci USA* 101:17528–17532
- Merkle FT, Mirzadeh Z, Alvarez-Buylla A (2007) Mosaic organization of neural stem cells in the adult brain. *Science* 317:381–384
- Merkle FT, Fuentealba LC, Sanders TA, Magno L, Kessar N, Álvarez-Buylla A (2014) Adult neural stem cells in distinct microdomains generate previously unknown interneuron types. *Nat Neurosci* 17:207–214
- Ming G-L, Song H (2011) Adult neurogenesis in the mammalian brain: significant answers and significant questions. *Neuron* 70:687–702
- Mirzadeh Z, Merkle FT, Soriano-Navarro M, Garcia-Verdugo J-M, Álvarez-Buylla A (2008) Neural stem cells confer unique pinwheel architecture to the ventricular surface in neurogenic regions of the adult brain. *Cell Stem Cell* 3:265–278
- Mirzadeh Z, Doetsch F, Sawamoto K, Wichterle H, Álvarez-Buylla A (2010) The subventricular zone en-face: wholemount staining and ependymal flow. *J Vis Exp* 39:1–8
- Muzumdar MD, Tasic B, Miyamichi K, Li L, Luo L (2007) A global double-fluorescent Cre reporter mouse. *Genesis* 45:593–605

- Nair KS, Hmani-Aifa M, Ali Z, Kearney AL, Salem SB, Macalinao DG, Cosma IM, Bouassida W, Hakim B, Benzina Z, Soto I, Söderkvist P, Howell GR, Smith RS, Ayadi H, John SWM (2011) Alteration of the serine protease PRSS56 causes angle-closure glaucoma in mice and posterior microphthalmia in humans and mice. *Nat Genet* 43:579–584
- Nolte C, Matyash M, Pivneva T, Schipke CG, Ohlemeyer C, Hanisch UK, Kirchhoff F, Kettenmann H (2001) GFAP promoter-controlled EGFP-expressing transgenic mice: a tool to visualize astrocytes and astrogliosis in living brain tissue. *Glia* 33:72–86
- Nunes MC, Roy NS, Keyoung HM, Goodman RR, McKhann G, Jiang L, Kang J, Nedergaard M, Goldman SA (2003) Identification and isolation of multipotential neural progenitor cells from the subcortical white matter of the adult human brain. *Nat Med* 9:439–447
- Palmer TD, Ray J, Gage FH (1995) FGF-2-responsive neuronal progenitors reside in proliferative and quiescent regions of the adult rodent brain. *Mol Cell Neurosci* 6:474–486
- Pencea V, Bingaman KD, Wiegand SJ, Luskin MB (2001) Infusion of brain-derived neurotrophic factor into the lateral ventricle of the adult rat leads to new neurons in the parenchyma of the striatum, septum, thalamus, and hypothalamus. *J Neurosci* 21:6706–6717
- Pierce AA, Xu AW (2010) De novo neurogenesis in adult hypothalamus as a compensatory mechanism to regulate energy balance. *J Neurosci* 30:723–730
- Reynolds BA, Tetzlaff W, Weiss S (1992) A multipotent EGF-responsive striatal embryonic progenitor cell produces neurons and astrocytes. *J Neurosci* 12:4565–4574
- Rivers LE, Young KM, Rizzi M, Jamen F, Psachoulia K, Wade A, Kessaris N, Richardson WD (2008) PDGFRA/NG2 glia generate myelinating oligodendrocytes and piriform projection neurons in adult mice. *Nat Neurosci* 11:1392–1401
- Robins SC, Stewart I, McNay DE, Taylor V, Giachino C, Goetz M, Ninkovic J, Briancon N, Maratos-Flier E, Flier JS, Kokoeva MV, Placzek M (2013a) α -Tanycytes of the adult hypothalamic third ventricle include distinct populations of FGF-responsive neural progenitors. *Nat Commun* 4:2049
- Robins SC, Trudel E, Rotondi O, Liu X, Djogo T, Kryzskaya D, Bourque CW, Kokoeva MV (2013b) Evidence for NG2-glia derived, adult-born functional neurons in the hypothalamus. *PLoS ONE* 8:e78236
- Rodríguez EM, Blázquez JL, Pastor FE, Peláez B, Peña P, Peruzzo B, Amat P (2005) Hypothalamic tanycytes: a key component of brain-endocrine interaction. *Int Rev Cytol* 247:89–164
- Seki T, Sato T, Toda K, Osumi N, Imura T, Shioda S (2013) Distinctive population of Gfap-expressing neural progenitors arising around the dentate notch migrate and form the granule cell layer in the developing hippocampus. *J Comp Neurol* 522:261–283
- Seri B, García-Verdugo JM, McEwen BS, Alvarez-Buylla A (2001) Astrocytes give rise to new neurons in the adult mammalian hippocampus. *J Neurosci* 21:7153–7160
- Sousa-Ferreira L, de Almeida LP, Cavadas C (2014) Role of hypothalamic neurogenesis in feeding regulation. *Trends Endocrin Met* 25:80–88
- Spassky N, Merkle FT, Flames N, Tramontin AD, Garcia-Verdugo J-M, Álvarez-Buylla A (2005) Adult ependymal cells are postmitotic and are derived from radial glial cells during embryogenesis. *J Neurosci* 25:10–18
- Stenman J, Toresson H, Campbell K (2003) Identification of two distinct progenitor populations in the lateral ganglionic eminence: implications for striatal and olfactory bulb neurogenesis. *J Neurosci* 23:167–174
- Tramontin AD, Garcia-Verdugo J-M, Lim DA, Álvarez-Buylla A (2003) Postnatal development of radial glia and the ventricular zone (VZ): a continuum of the neural stem cell compartment. *Cereb Cortex* 13:580–587
- Urbán N, Guillemot F (2014) Neurogenesis in the embryonic and adult brain: same regulators, different roles. *Front Cell Neurosci* 8:396
- Xu Y, Tamamaki N, Noda T, Kimura K, Itokazu Y, Matsumoto N, Dezawa M, Ide C (2005) Neurogenesis in the ependymal layer of the adult rat 3rd ventricle. *Exp Neurol* 192:251–264
- Young KM, Fogarty M, Kessaris N, Richardson WD (2007) Subventricular zone stem cells are heterogeneous with respect to their embryonic origins and neurogenic fates in the adult olfactory bulb. *J Neurosci* 27:8286–8296
- Zhao C, Deng W, Gage FH (2008) Mechanisms and functional implications of adult neurogenesis. *Cell* 132:645–660